SHAKE TABLE TEST AND NUMERICAL SIMULATION ON SEISMIC RESPONSES OF RAISED FLOOR

W.I. Liao[1] and J.F. Chai[2]

[1] *Associate Professor, Dept. of Civil Engineering, Taipei University of Technology, Chinese Taiwan*
[2] *Research Fellow, Center for Research on Eqrthquake Engineering (NCREE), Chinese Taiwan*
Email: wiliao@ntut.edu.tw, jfchai@ncree.org

ABSTRACT :

This paper presents the seismic performance of raised floor system by shake table excitations. The tested raised floor system was assembled by 7x7 panels with pedestal-stringer frame structure, supporting a simulated equipment with varies weight and geometry shape, the size of the panel is 60x60 cm, the height of the pedestal is 45 cm. This raised floor system was the typical system that frequently used in Taiwan semi-conductor FAB. The input motions for the shake table tests were the waffle-slab floor acceleration responses of a typical semi-conductor FAB by input simulated ground motions. The dynamic characteristics include the acceleration amplification and dependence of input motions by raised floor system was studied and discussed. This study also employee the finite element package to carry out numerical simulation on seismic responses of raised floor systems and compared with the experimental data, and show that the proposed simulation model was very excellent.

KEYWORDS: high-tech FAB, seismic performance, base isolation, numerical simulation

1. INTRODUCTION

Seismic performance of nonstructural elements such as the raised floor system has not attracted much attention. However, damage of expensive equipments that stand in the raised floor system of high-tech FAB was often observed during past earthquake in Taiwan area. This will results in huge loss of manufacturing functions and properties for the high-tech FAB. Therefore, there is need to understand the dynamic performance of the raised floor system for future seismic protection. For hi-tech industry, the equipments stand on raised floor system should be designed to withstand the effects of a considerable earthquake without any loss of the capacity to perform their functions. For such equipments, a separate analysis can be implemented using the floor acceleration time-history excitations at the supported locations derived from the analysis of the supporting structure. Therefore, the first objective of this study is to generate the input ground motions consistent with the maximum potential earthquake for the supporting structure. Then, the horizontal floor acceleration responses at interesting supported locations can be developed from the time-history motions resulted from dynamic analysis of the supporting structure, and these floor responses are adopted for the dynamic analysis and shake table test of the equipment-raised floor system supported by the supporting structure. In this study, a pedestal-stringer-frame raised floor system supporting a simulated equipment was tested using the shake table to understand its dynamic characteristics. The tested raised floor system was a typical system that frequently used in Taiwan semi-conductor FAB. The simulated ground motions are base on the phase spectrum and the maximum potential earthquake of site located at Taiwan Hsin-Chu Science Park. The dynamic characteristics include the acceleration amplification and dependence of input motions by raised floor system was studied and discussed. Numerical simulation also carries out to study dynamic responses of raised floor systems and compared with the test data.

2. MAXIMUM POTENTIAL EARTHQUAKE

This study is focused on the hi-tech Fabs located at the Hsin-Chu Science Park, and hence, the seismic hazard analysis for this target site is performed firstly. Based on the de-aggregation method, the maximum potential magnitude and hypocentral distance of the earthquake with a return period of 475 years can be determined as Mc=6.4and Rc=17.6 km. Then, based on the attenuation laws of spectral acceleration demands for a hard site, the associated spectral response accelerations at short period (0.3 sec.) and at 1 second can be predicted as S_{aS}=0.32g and S_{a1}=0.17g. Therefore, the uniform hazard response spectrum corresponding to the maximum potential earthquake for Hsin-Chu Science Park can be developed by

$$S_{aD} = \begin{cases} S_{as}\left(0.4 + 3T/T_0\right) & ; \quad T \le 0.2T_0 \\ S_{as} & ; \quad 0.2T_0 < T \le T_0 \\ S_{a1}/T & ; \quad T_0 < T \end{cases} \tag{2.1}$$

where T is the fundamental period of the structure in the unit of second, and T_0=S_{a1}/S_{aS} is the corner period between the short and moderate-to-long period ranges. The shape of response spectrum is shown in Fig. 1.

3. PHASE SPECTRUM

For the time-history analysis of the structure, the input ground motions consistent with the maximum potential earthquake should be simulated. For a target site, the most important issue is to model the phase spectrum because the phase characteristic of an earthquake strongly controls the non-stationary nature of earthquake motions. As long as the phase spectrum corresponding to the maximum potential earthquake can be modeled, the input ground motions can be simulated by modifying the Fourier amplitude from the available response spectrum. Therefore, the simulated ground motion will be compatible with the response spectrum and perform the same waveform characteristics as the maximum potential earthquake observed at the target site.

Group delay time is defined as the derivative of the phase spectrum with respect to the circular frequency. The mean value of group delay time and its standard deviation within a certain frequency range represent the central arrival time and duration, respectively, of the earthquake motion with frequency content in such a bandwidth. Therefore, it is much easier to model the group delay time than to model the phase spectrum directly. In this study, the phase spectrum is modeled one by one for a series of separate frequency bands corresponding to the Meyer wavelet decomposition. Furthermore, based on the statistical analysis, it can be found that the student t-distribution with a degree of freedom ϕ=3 can be recognized as the representative distribution of group delay times within a compact support (Chai *et al.* 2002). Therefore, for a given set of mean value and standard deviation of group delay times for a certain frequency range, the sample of group delay times at each discrete frequency within the frequency range can be generated randomly by the identified probability density function of the student t-distribution (ϕ=3), and further, the phase spectrum can be modeled by integrating the generated group delay times.

The mean value $\mu_{tgr}^{(j)}$ and standard deviation $\sigma_{tgr}^{(j)}$ of group delay times for each decomposed component can be modeled as functions of the earthquake magnitude (M) and the hypocentral distance (R) by:

$$\begin{aligned} \mu_{tgr}^{(j)} &= \alpha_1^j \times 10^{\beta_1^j M} \times R^{\gamma_1^j} \\ \sigma_{tgr}^{(j)} &= \alpha_2^j \times 10^{\beta_2^j M} \times R^{\gamma_2^j} \end{aligned} \tag{3.1}$$

The parameters should be regressed by the observed earthquake data sets. In this study, the ground motions observed at the CWB stations (TSMIP) which are located at the hard site surrounding the target site (total 27 stations) are considered as the candidates firstly. Then, the further criteria are defined by PGA ≥ 5 gal, duration ≥ 40 sec and the motions should be induced by the crustal earthquakes with M_L ≥ 4.0. As a result, there are total 276 ground motions for 65 earthquake events are selected for the regress analysis. Figure 2 shows the locations of the target site and its surrounding CWB stations as well as the epicenters of selected earthquake events.

For each ground motion, based on the azimuth angle between the epicenter and the observation point, the EW- and NS- components can be transformed to the longitudinal and transverse directions. Then for the longitudinal and transverse components separately, the phase spectrum of each wavelet decomposed signals can be determined, and further, the associated mean value and standard deviation of group delay times within the specified frequency range can be carried out straightforwardly. Therefore, based on the mean values and standard deviations of group delay times within a certain frequency range determined from all of the selected earthquake data with given pairs of M and R, the parameters in Eqn. 3.1 can be regressed for each decomposed component by means of the least square method, and they are determined for both the longitudinal and transverse directions independently.

Hence, based on the regressed empirical function as well as the maximum potential magnitude and distance determined by de-aggregation method for the target site, the associated mean value and standard deviation of group delay times can be predicted for each specified frequency range. Then, as mentioned before, the sample of group delay times at each discrete frequency within the frequency range can be generated randomly by the identified probability density function of the student t-distribution (ϕ=3), and further, the phase spectrum corresponding to the maximum potential earthquake can be modeled by integrating the generated group delay times.

4. SPECTRUM COMPATIBLE INPUT MOTIONS

In addition to the modeling of phase spectrum, the Fourier amplitude should be determined to simulate the maximum potential input ground motion. Based on the modeled phase spectrum and a trial Fourier amplitude $A_m(\omega)$, the total ground motion can be recovered and then the associated spectral response acceleration $S_{am}(T)$ for any structural period T can be determined. Because the structural response will be dominated by the wave with resonant frequency, the modification factor for the Fourier amplitude at a circular frequency of ω=2π/T can be defined by

$$MF_m(\omega)\big|_{\omega=2\pi/T} = S_{aD}(T)/S_{am}(T) \tag{4.1}$$

where $S_{aD}(T)$ is the spectral acceleration demand at period T corresponding to the maximum potential earthquake. Then, the Fourier amplitude $A_{m+1}(\omega)$ on the next iteration can be defined by

$$A_{m+1}(\omega) = MF_m(\omega) \times A_m(\omega) \tag{4.2}$$

This iteration process will be continued until $MF_m(\omega)$ is equal to 1.0 at all frequencies. The final recovered ground motions will be compatible with the response spectrum corresponding to the maximum potential earthquake and perform the waveform characteristics at the target site. The simulated time-histories of ground acceleration in the longitudinal direction is shown in Fig. 3. In addition, it can be found that the associated response spectrum is in good compatible condition with the response spectrum corresponding to the maximum potential earthquake.

5. FLOOR RESPONSES OF FAB

The horizontal floor responses at interesting locations can be developed from the time-history motions resulted from the dynamic analysis of the supporting structure. Figure 4 show the plane view and section view of a typical semiconductor FAB in Taiwan, and this structure is adopted in this study for to compute the floor acceleration responses at interesting locations. In general, for to have a widely manufacturing space, the clean room is shield by a long span mega steel truss that stands on a very rigid RC shear wall. The slab of clean room is very stiff waffle slab supported by close columns and very rigid shear walls for control the micro vibration to meet the micro-vibration criteria (Keith and Chris, 1999; Gordon, 1991). In this study, the waffle slab is modeled by a general plate element with thickness and coefficients being identified to satisfy the conditions that

the total mass, boundary condition and the associated frequencies of the diaphragm will be same as those modeled by grid elements. On the other hand, the other elements and components such as the RC beams, columns, joints, shear walls and the steel trusses are modeled by the associated elements as prepared in SAP2000. For the selected FAB structure of this study, the fundamental and second frequencies in space mega truss direction are determined as 3.3 Hz and 6.2 Hz, respectively. The modal mass of first mode major from the vibration of space truss, and the modal mass of second mode major from the vibration of clean room story. These vibration frequencies are verified by the identification result of ambient test.
Based on the simulated input ground motions consistent with the maximum potential earthquake with a return period of 475 years, the time-history of the response at each representative location can be determined and used to as the input motions of the shake table test of raised floor system. Figure 5 shows the acceleration response at center of the clean-room story. Figure 6 shows the response spectrum that by floor acceleration response. It can be found that the peak spectral response appears coincidently at the fundamental frequency of supporting structure, and the contribution of acceleration response from second mode is higher than the first mode.

6. DYNAMIC RESPONSES OF RAISED FLOOR SYSTEM

A steel based pedestal-stringer-frame raised floor system is adopted for the shake table test. The plane size of the raised floor system is 4.2mx4.2m, and the height of pedestal of raised floor is 60cm. The inner and outer diameters of the pedestal tube are 4.8cm and 5.2cm, respectively. Aluminum-alloy panel is 60x60 cm with ultimate vertical capacity of 300kgf. The panel and stringer are bolted on the top supporting base of pedestal. Figure 7 shows the test setup of the raised floor system. A steel frame with additional mass blocks for modeling the equipment is stand on the raised floor. Three cases of assemblage of mass blocks in the steel frame are adopted in this test and shown in Table 1. For to archiving the acceleration amplification of input motions by the raised floor system, an identical steel frame was directly installed on the concrete slab just beside the raised floor system for comparison. The location of accelerometers and strain gauges is shown in Figure 8. The input motions of the shake table test are those floor acceleration responses obtained in previous section. Corresponding to the input motion, the test protocol is sequentially the peak ground acceleration (PGA) of 200gal, 400gal, and with an increment of approximately 200gal for next test run until 1000gal for case B1, and PGA of 200 gal and 600 gal for case B2 and B3. During the test, the readings of all strain gauges on the pedestal are far below the yield strain. That means the pedestals are remaining in the elastic range even the PGA reach 1000gal.

Figures 9a-9c show the relation between the PGA measured by accelerometer and the PGA of input motion. From these figures we can found that the amplification ratios of PGA of case B1 and B2 are approximately have the same values, but for case B3, its PGA amplification ratio is more higher than case B1 and B2 because steel frame of case B3 has higher vibration frequency and its frequency close to the fundamental frequency of raised floor. For the case B1 responses, the amplification ratio of PGA of accelerometer A3 is approximately keep in 4.0 from lowest input PGA=0.2 g to highest input PGA=1 g, that means the system used in this test may remain in elastic range.

Figure 10 shows the modeling of the raised floor system and its supporting equipment. The pedestal, stringer and panel are modeled by the associated elements as prepared in SAP2000. The fundamental frequency of the raised floor system is 21.5 Hz by analysis; it is very close to frequency 22 Hz that identify from shake table test. Figure 11 shows the comparison of the acceleration time history between simulation and test. Only the time interval 5-20 seconds has shown in this figure for easy to demonstrate the comparison. It can be found the agreement of acceleration response is excellent.

7. CONCLUSION

This paper proposes a separated and comprehensive study procedure of high raised floor system in a typical FAB structure. The input ground motions are generated base on the phase spectrum and the maximum potential earthquake of site located at Taiwan Hsin-Chu Science Park. Then, the horizontal floor acceleration responses at interesting locations are computed from dynamic analysis of the supporting structure, and these floor responses are used for the shake table test and dynamic analysis of the equipment-raised floor system. The tested raised floor system was a typical system that frequently used in Taiwan semi-conductor FAB. The dynamic characteristics include the acceleration amplification and dependence of input motions by raised floor system was studied and discussed.

ACKNOWLEDGEMENTS

The authors gratefully acknowledge the financial support granted by the Science Council (NSC). The facilities for research provided by Center for Research on Earthquake Engineering (NCREE) are also highly appreciated.

REFERENCES

Chai, J.-F., C.-H. Loh, and T. Sato, (2002). Modeling of Phase Spectrum to Simulate Design Ground Motions. *Journal of the Chinese Institute of Engineers*, **25:4,** 447-459.

Keith, W.L. and Chris, A.P., (1999). Micro-vibration criteria for 300 mm and beyond. Semiconductor FABTECH, 10th edition, 167-170.

Gordon, C.G., (1991), Generic criteria for vibration sensitive equipment, Vibration control in microelectronic, optics and metrology. SPIE Proceedings, **1619**, 71-85.

Table 1 Three cases of mass block allocation

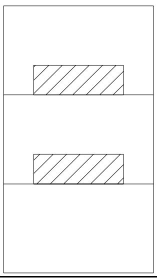	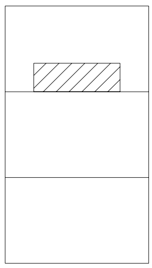	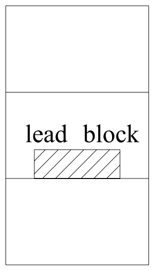
Case B1	Case B2	Case B3

Weight of lead blocks = 250kgf

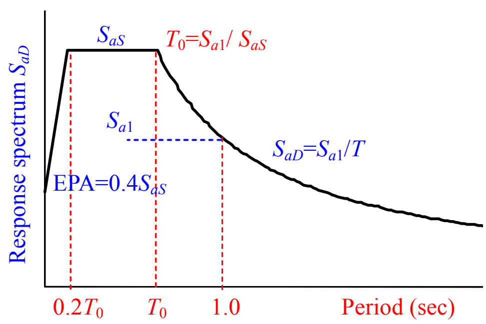

Figure 1 Structural response spectrum corresponding to the maximum potential earthquake

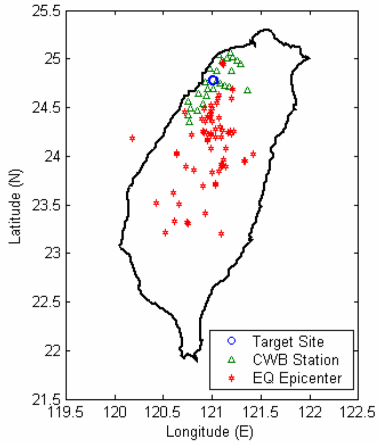

Figure 2 Map of the CWB stations and the epicenters of earthquake events selected for regress analysis

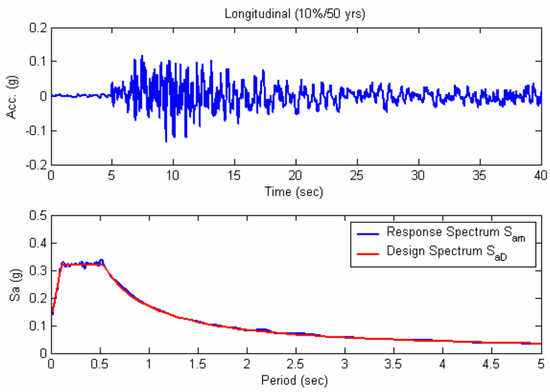

Figure 3 Simulated longitudinal ground acceleration and response spectrum corresponding to the maximum potential earthquake with a return period of 475 years.

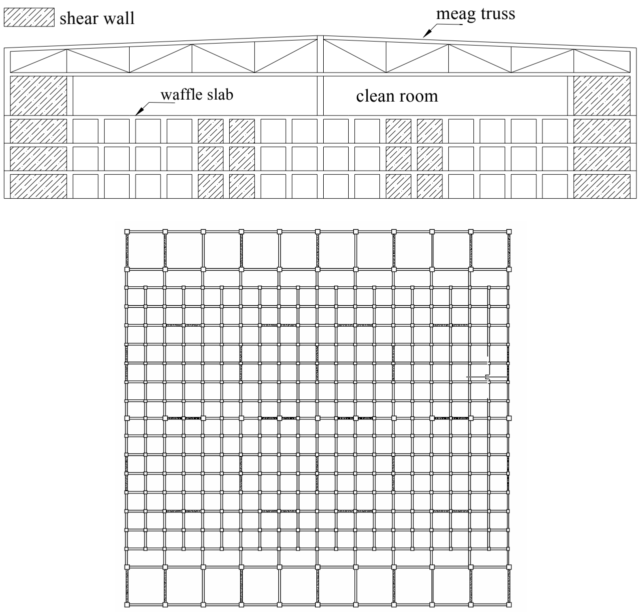

Figure 4 Section view and clean-room plane view of a typical FAB structure.

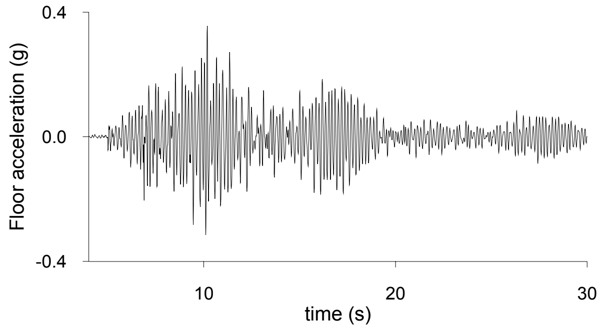

Figure 5 Floor acceleration response at clean-room

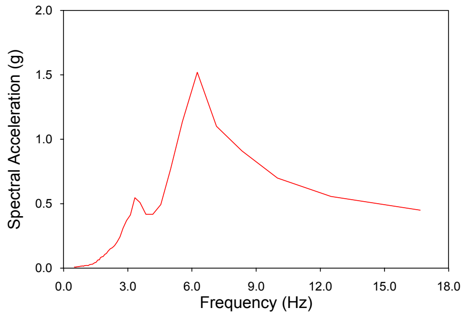

Figure 6 Normalized floor response spectra as excited in truss direction (Y-direction).

Figure 7 Test setup of the raised floor system.

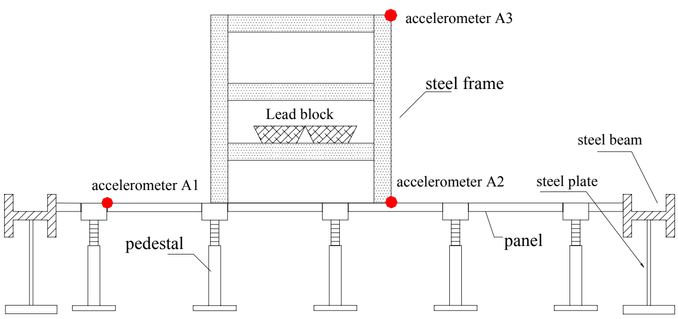

Figure 8 Test Configuration and locations of accelerometers.

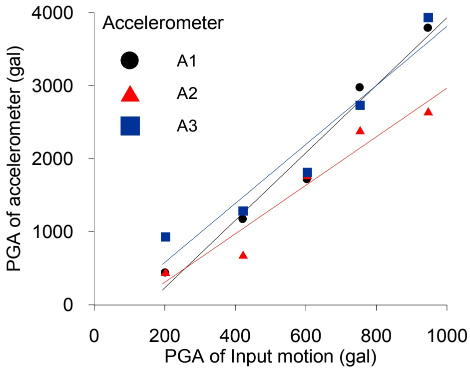

Figure 9a Relation of PGA of input and output for case B1.

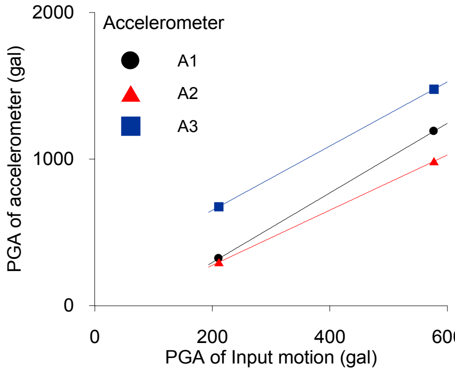

Figure 9b Relation of PGA of input and output for case B2.

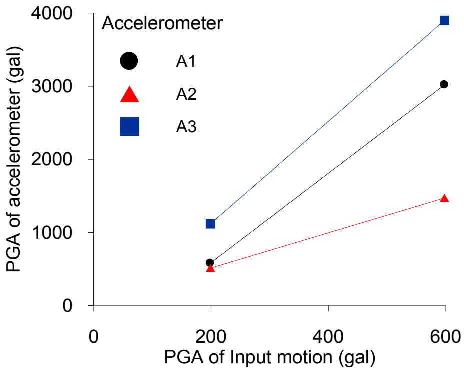

Figure 9c Relation of PGA of input and output for case B3.

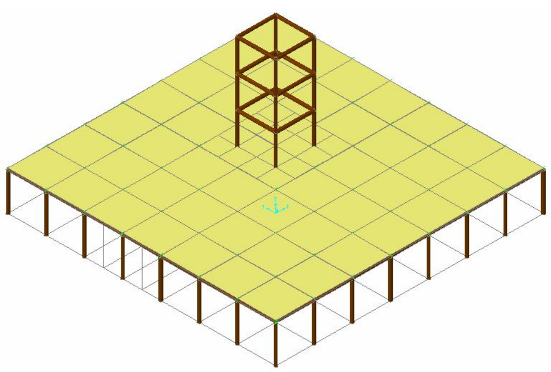

Figure 10 Numerical model of raised floor system

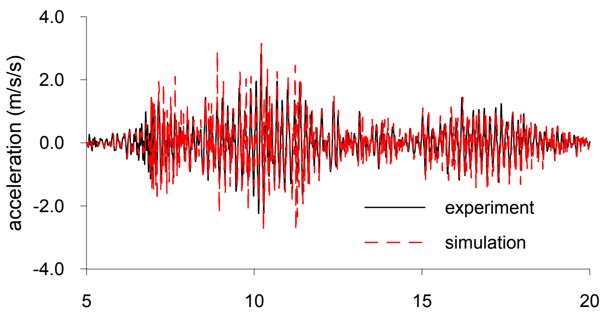

Figure 11 Comparison of simulated and experimental acceleration response